Liquid Crystals
Publication details, including instructions for authors and subscription information:
http://www.informaworld.com/smpp/title~content=t713926090

Invited Lecture. Molecular order and motion in nematogens from pulsed dynamic N.M.R. A comparative study of model compounds and parent liquid-crystal polymers

K. Kohlhammer[a]; K. Müller[a]; G. Kothe[a]
[a] Institut für Physikalische Chemie, Universität Stuttgart, Stuttgart, F. R. Germany

To cite this Article Kohlhammer, K. , Müller, K. and Kothe, G.(1989) 'Invited Lecture. Molecular order and motion in nematogens from pulsed dynamic N.M.R. A comparative study of model compounds and parent liquid-crystal polymers', Liquid Crystals, 5: 5, 1525 — 1547
To link to this Article: DOI: 10.1080/02678298908027789
URL: http://dx.doi.org/10.1080/02678298908027789

LIQUID CRYSTALS, 1989, VOL. 5, NO. 5, 1525–1547

Invited Lecture

Molecular order and motion in nematogens from pulsed dynamic N.M.R.

A comparative study of model compounds and parent liquid-crystal polymers

by K. KOHLHAMMER, K. MÜLLER and G. KOTHE
Institut für Physikalische Chemie, Universität Stuttgart, Pfaffenwaldring 55, D-7000 Stuttgart 80, F.R. Germany

Model compounds of semiflexible liquid-crystal polymers (LCPs), specifically deuteriated at various positions of the mesogenic units and aliphatic chains, have been studied by multipulse dynamic N.M.R. techniques. Analysis of the various experiments, employing a density-matrix treatment based on the stochastic Liouville equation, provides new information about the dynamic organization of the different systems. The results, referring to monomers and dimers, are discussed in relation to the properties of the parent LCPs.

The pronounced increase in orientational order from the monomers to the dimers can be rationalized by an intramolecular order transfer via highly extended spacers, in agreement with observations for the parent LCPs. A strong dependence of the nematic order on the parity of the spacer (even–odd effect) supports this concept. However, long-range orientational order of both model compounds is completely lost upon crystallization. Thus, despite the fact that dimers already achieve unusually high order parameters in the nematic phase, many of the exceptional properties of LCPs are restricted to systems with higher molecular weights.

Molecular motions in the model compounds occur within an extremely broad dynamic range, extending from 10^{-12} s (internal reorientation) in the fast-rotational to 10^{-3} s (director order fluctuations) in the ultraslow-motion regime. With respect to these dynamic properties, dimers behave like conventional monomeric liquid crystals, exhibiting much faster motions than the polymers.

1. Introduction

Semiflexible liquid-crystal polymers (LCPs) are of considerable current interest, both because of their theoretical and technological aspects. The occurrence of thermotropic mesophases in bulk polymers presents a challenging theoretical problem [1–3]. The ease with which these polymers can be oriented has been employed in the formation of fibres with unusually high tensile strengths and moduli [4]. Apparently, semiflexible LCPs exhibit distinctive mesophase properties, studied by a variety of experimental techniques [4–15]. Among these, pulsed N.M.R. has played an important role in the elucidation of the dynamic organization of these systems [4, 8–15]. The most prominent results from these studies are exceptionally high order parameters, exceeding those of conventional liquid crystals by a considerable amount. Moreover, the order parameters are quantitatively retained when the polymers are cooled into

0267–8292/89 $3.00

the solid state. Apparently, the mesomorphic behaviour of semiflexible LCPs differs from that of the monomeric analogues.

Model calculations based on statistical-mechanical theories led to the notion that dimers, consisting of two mesogenic units linked by a flexible spacer, reliably reflect the liquid-crystalline properties of the polymers [2, 16]. A variety of such dimeric model compounds has already been prepared [17–24]. However, while considerable interest has centred on the synthetic design and macroscopic behaviour of the systems, relatively little attention has been focused on the dynamic and structural features of the molecular units. So far, the details of the molecular motion in the liquid-crystalline state are unknown. Moreover, there is only limited information about the orientational order of the mesogenic units and the conformational order of the spacer [21–24].

In the present study we investigate these molecular properties with deuteron (^{2}H) N.M.R., employing multipulse techniques. Variation of pulse sequence, pulse separation, magnetic-field orientation and magnetic field strength provides the large number of independent experiments, necessary for a proper molecular characterization of the systems. In section 2 of this paper the theoretical background is presented. This theory is then applied to the analysis of dynamic ^{2}H N.M.R. experiments of specifically deuteriated model compounds (monomers and dimers), derived from semiflexible polyesters. Computer simulations provide the orientational distributions and conformations of the molecular units and the correlation times of the various motions. They are compared with the molecular order and dynamics of the parent LCPs.

2. Theory

Analysis of the dynamic ^{2}H N.M.R. experiments is performed in terms of the density-operator formalism, outlined elsewhere [13, 25]. Here we summarize the important features of this approach and introduce the simulation parameters. The spin hamiltonian $H(\Omega)$, representing Zeeman and quadrupole interactions in the laboratory frame (**x**, **y**, **z**) is conveniently written as

$$H(\Omega) = \hbar\omega_0 I_z + \sum_{m=-2}^{2} (-1)^m F_{2,-m}(\Omega) T_{2,m}, \tag{1}$$

where $\omega_0 = -\gamma B_z$ is the Larmor frequency of the spin systems, and $T_{2,m}$ and $F_{2,-m}$ denote laboratory-frame spin operators and spatial operators respectively. Generally, non-secular terms, $T_{2,m}$ with $m \neq 0$, have to be retained in the analysis. The orientation dependence of the spatial operators can be evaluated by a threefold transformation from the magnetic-tensor system ($\mathbf{X}_K$, $\mathbf{Y}_K$, $\mathbf{Z}_K$), in which

$$\left.\begin{aligned} F'_{2,0} &= \tfrac{1}{4}6^{-1/2}e^2qQ, \\ F'_{2,\pm 1} &= 0 \\ F'_{2,\pm 2} &= \tfrac{1}{4}e^2qQ\eta, \end{aligned}\right\} \tag{2}$$

and e^2qQ and η denote the quadrupole coupling constant and asymmetry parameter respectively. In the first step we transform to a molecular coordinate system ($\mathbf{X}_M$, $\mathbf{Y}_M$, $\mathbf{Z}_M$), using the Wigner rotation matrix $\mathbf{D}^{(2)}(\phi_K\theta_K\psi_K)$. In the second and third step we rotate by the Euler angles (ϕ_M, θ_M, ψ_M) and (Φ, Θ, Ψ) into the laboratory frame (figure 1) and obtain

$$F_{2,m}(\Omega) = \sum_{m',m'',m'''=-2}^{2} D^{(2)}_{m'm}(\Phi\Theta\Psi) D^{(2)}_{m''m'}(\phi_M\theta_M\psi_M) D^{(2)}_{m'''m''}(\phi_K\theta_K\psi_K) F'_{2,m'''}. \tag{3}$$

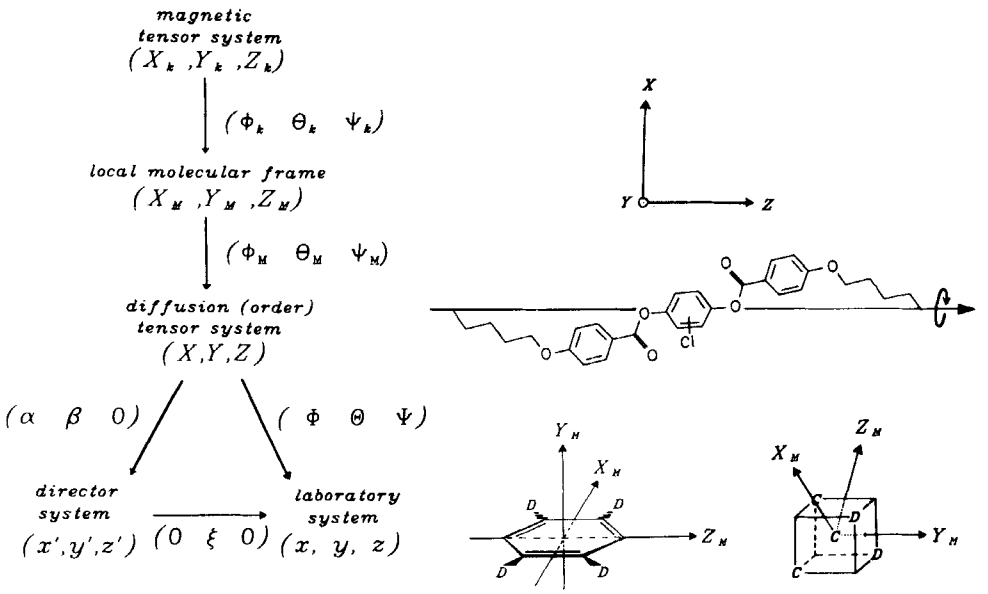

Figure 1. Notation for coordinate systems and Euler transformations used in the N.M.R. relaxation model. The various coordinate systems are as follows: magnetic-tensor system ($\mathbf{X}_K$, $\mathbf{Y}_K$, $\mathbf{Z}_K$) ($\mathbf{Z}_K$ = C–D bond direction); local molecular frame ($\mathbf{X}_M$, $\mathbf{Y}_M$, $\mathbf{Z}_M$) ($\mathbf{Z}_M$ = *para* axis for phenyl deuterons; $\mathbf{Z}_M$ = direction of *trans*-configurated alkyl chain); diffusion- (order-) tensor system (**X**, **Y**, **Z**) (**Z** = long axis of molecule or repeating unit respectively); director system (**x**′, **y**′, **z**′) (**z**′ = net ordering axis of molecule or repeating unit); laboratory system (**x**, **y**, **z**) (**z** = magnetic-field direction). The definitions of the Euler angles are given in [13, 25].

In order to describe the time evolution of the density matrix $\varrho(t)$ during some arbitrary pulse sequence, we divide the sequence into regions where a pulse is present and regions where there is no pulse. The action of the different non-selective pulses is considered by unitary transformations employing Wigner rotation matrices [13, 25]. Between the pulses, the density matrix is assumed to obey the stochastic Liouville equation [26, 27]

$$\frac{\partial}{\partial t}\varrho(\Omega, t) = -\frac{i}{\hbar}\mathbf{H}^{\times}(\Omega)\cdot\varrho(\Omega, t) - \Gamma_{\Omega}\cdot[\varrho(\Omega, t) - \varrho_{eq}(\Omega)], \tag{4}$$

which we solve using a finite-grid-point method [28, 29]. Here $\mathbf{H}^{\times}(\Omega)$ denotes a super-operator associated with the spin hamiltonian $H(\Omega)$. Γ_{Ω} is the stationary Markov operator for the various rotational processes and $\varrho_{eq}(\Omega)$ is the equilibrium density matrix.

In the finite-grid-point method [28, 29], the Markov operator is represented by a matrix $\mathbf{W}(\Omega, \Omega)$ whose elements give the transition rates between discrete sites of Ω. The values of the transition rates depend upon the model used to describe the motion. For the intramolecular dynamics (*trans–gauche* isomerization, ring flips) a random jump process is assumed. Consequently [30],

$$W(\Omega_m, \Omega_n) = \tau_J^{-1}[P_{eq}(\Omega_n) - \delta_{mn}], \tag{5}$$

where τ_J is the average residence time in one conformation. For the intermolecular motion (overall reorientation), rotation through a sequence of infinitesimally small

angular steps is assumed. In that case the elements of $\mathbf{W}(\Omega, \Omega)$ must satisfy the following equations [31]:

$$\left.\begin{aligned} W(\Omega_m, \Omega_{m+1}) + W(\Omega_m, \Omega_{m-1}) &= (3\Delta^2\tau_R)^{-1}, \\ W(\Omega_m, \Omega_n)P_{eq}(\Omega_m) &= W(\Omega_n, \Omega_m)P_{eq}(\Omega_n), \\ W(\Omega_m, \Omega_m) &= -(3\Delta^2\tau_R)^{-1}, \end{aligned}\right\} \quad (6)$$

where Δ is the angular separation of adjacent grid points. Solving equation (6), one can establish values for all intermolecular transition rates in terms of two rotational correlation times $\tau_{R\perp}$ and $\tau_{R\parallel}$ and the equilibrium population $\mathbf{P}_{eq}(\Omega)$ of the sites; $\tau_{R\perp}$ is the correlation time for reorientation of the symmetry axis of the diffusion tensor, while $\tau_{R\parallel}$ refers to rotation about this axis.

The equilibrium distribution $\mathbf{P}_{eq}(\Omega)$ is described in terms of internal and external coordinates. The internal part accounts for different conformations and the external part for different orientations. Generally, there are only four conformational states for a particular aliphatic chain segment [32]. The corresponding populations n_1, n_2, n_3 and n_4 may be used to set up a segmental order matrix, which on diagonalization yields the segmental order parameters $S_{Z'Z'}$ and $S_{X'X'} - S_{Y'Y'}$ [25]. They respectively express the ordering of the most-ordered segmental axis $\mathbf{Z}'$ and the anisotropy of that order.

The external part of the equilibrium distribution is described in the mean-field approximation, using an orienting potential such as is common in molecular theories of liquid crystals. In the case of uniaxial phases only two adjustable parameters, A_{00} and A_{20}, enter the orientational distribution function [33]:

$$f(\Phi\Theta\Psi) = N \exp\{A_{00}D^{(2)}_{00}(0\beta 0) + A_{20}[D^{(2)}_{20}(\alpha\beta 0) + D^{(2)}_{-20}(\alpha\beta 0)]\}. \quad (7)$$

In expressing the Wigner elements $D^{(2)}_{m0}(\alpha\beta 0)$ as functions of Φ, Θ, Ψ, we assume that the order tensor is colinear with the diffusion tensor. The coefficients A_{00} and A_{20} characterize the orientation of the molecules with respect to a local director $\mathbf{z}'$ while the angle ξ (figure 1) specifies the orientation of $\mathbf{z}'$ in the laboratory frame. The orientational order parameters S_{XX}, S_{YY} and S_{ZZ} are related to the coefficients A_{00} and A_{20} by mean-value integrals [33].

3. Experiments and methods

3.1. *Syntheses and preparations*

The model compounds and parent LCPs [34, 35] that we consider in detail have the molecular structures shown in figure 2. The acronyms **M1–P6** refer to fifteen different compounds, specifically deuteriated at the sites indicated in the formulae. Molecular weights $\bar{M}_n$ were determined by vapour-pressure osmometry, using tetrachloroethane as solvent. The phase behaviour of the liquid crystals was investigated by differential-scanning calorimetry (Perkin Elmer DSC-7) and polarization microscopy (Leitz Ortholux II, Linkham THM 600 hot stage). Table 1 lists the relevant thermodynamic properties. Apparently, all systems exhibit broad nematic phases. Note the two groups of dimers/polymers, which differ only in the aliphatic spacer, containing ten (**D1/P1–D3/P3, P4**) and nine segments (**D5/P5, D6/P6**) respectively.

Deuteron spin-labels were either attached to the mesogenic units or to various positions of the alkyl groups, as described elsewhere [36, 37]. Here we briefly outline the syntheses of the model compounds, prepared according to the general scheme shown in figure 3.

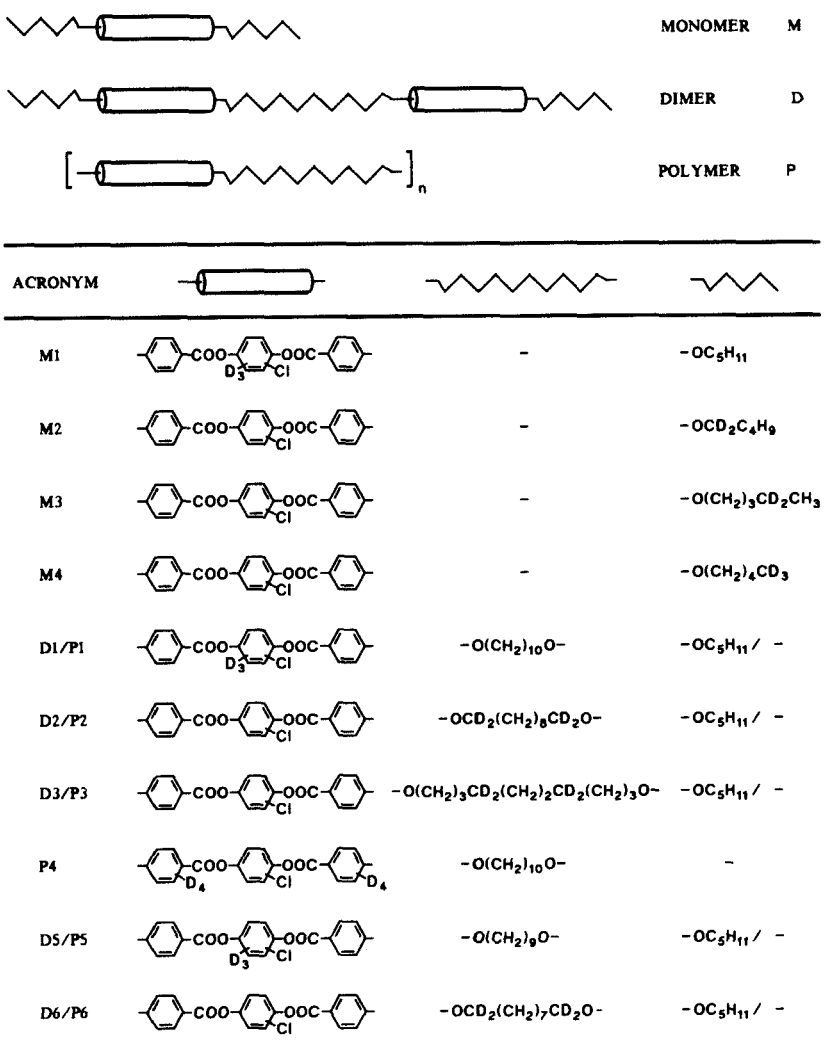

Figure 2. Molecular structures of selectively deuteriated model compounds **M**, **D** and corresponding parent liquid-crystal polymers **P**. Note that **D5/P5** and **D5/P6** differ from **D1/P1** and **D2/P2** only by the length of the flexible spacer.

Table 1. Physical properties of the model compounds and parent liquid-crystal polymers.

Liquid-crystal system	Spacer length	Molecular weight $\bar{M}_n$	Phase-transition temperature		Transition enthalpy	Transition entropy
			T_{cn}/K	T_{ni}/K	ΔH_{ni}/kJ mol^{-1}	ΔS_{ni}/J/(mol K)
M1–M4	—	525	369·5	454·4	2·1	4·6
D1–D3	10	1048	403·0	507·9	4·1	8·0
P1–P4	10	12000	430	552	6.7	12·1
D5, D6	9	1034	377·5	508·4	3·1	6·1
P5, P6	9	12000	429	543	6·5	11·8

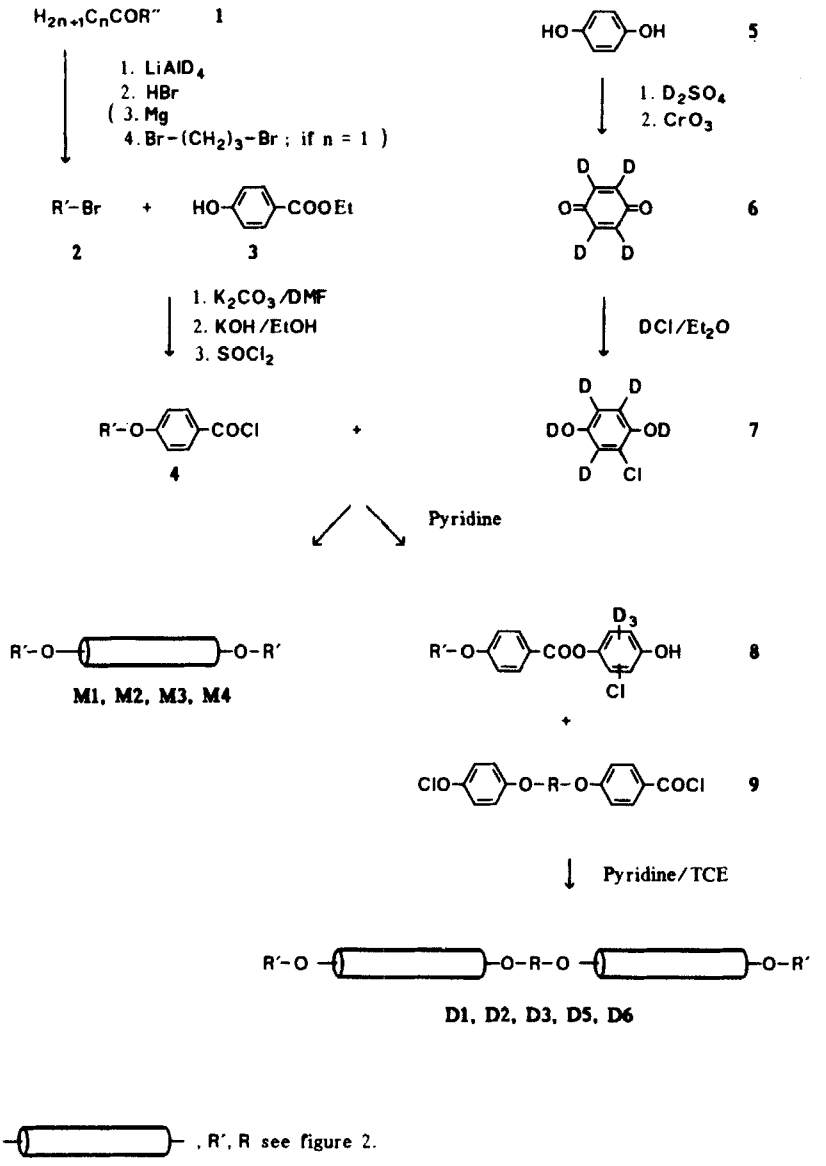

Figure 3. General scheme representing the synthetic pathway to the specifically deuteriated model compounds. Detailed descriptions of the syntheses are given in [36, 37].

The deuteriated alkyl groups of the monomers are generally prepared from the corresponding esters or acyl chlorides (**1**) by reduction with $LiAlD_4$, followed by bromination of the alcohols. In case of $n = 4$, formation of (**2**) is completed, while for $n = 1$ an additional Grignard reaction with 1,3-dibromopropane leads to the desired C_5 unit. Deuteriation of the terminal methyl group (**M4**) is achieved by employing commercial $D_3C–CH_2–Br$ (MSD Isotopes Inc.) and omitting the first steps (reduction and bromination). The bromides (**2**) are then attached to ethyl *p*-hydroxybenzoate (**3**) by a Williamson-type ether synthesis. Hydrolysis of the products and reaction with $SOCl_2$ yields the acid chlorides (**4**).

Deuteriation of the central phenyl ring is achieved by multiple H–D exchange of the hydroquinone (**5**) with D_2SO_4. Subsequent oxidation with CrO_3, according to literature procedures [38], yields the quinone (**6**), which is then converted into (**7**) by reaction with a solution of DCl in Et_2O at 0°C and by stirring for several hours at room temperature.

The acid chlorides (**4**) and chlorohydrochinones (**7**) are reacted either in a 2 : 1 molar ratio to yield the monomers **M1–M4** or in a 1 : 5 molar ratio to yield the dimer precursors (**8**). Addition of the acid chlorides (**4**) finally leads to the formation of the dimers **D1**, **D2**, **D3**, **D5** and **D6**, differing in length and specific deuteriation of the aliphatic spacer R. After purification by dry-column chromatography, the final products were characterized by elemental analysis, N.M.R. (^{13}C and ^{1}H) and mass spectrometry. The degree of deuteriation was found to be $\geqq 98$ per cent in the alkyl groups and $\geqq 95$ per cent in the aromatic rings.

Samples were prepared from 250 mg of deuteriated material in Wilmad N.M.R. tubes and sealed under vacuum for the N.M.R. measurements. Macroscopic alignment was achieved with a magnetic field of $B_z = 7{\cdot}0$ T in the nematic phase. After the N.M.R. measurements, the samples were checked for any degradation.

3.2. *Measurements and computations*

The ^{2}H N.M.R. experiments were performed on Bruker CXP 300 and MSL 300 spectrometers at 46·1 MHz, using quadrupole echo, $(\frac{1}{2}\pi)_x - \tau_1 - (\frac{1}{2}\pi)_y$, inversion recovery, $\pi - \tau_1 - (\frac{1}{2}\pi)_x - \tau_2 - (\frac{1}{2}\pi)_y$, and saturation recovery sequences $\frac{1}{2}\pi - \tau_1 - (\frac{1}{2}\pi)_x - \tau_2 - (\frac{1}{2}\pi)_y$. The width for a $\frac{1}{2}\pi$ pulse was 2·0 μs, employing a home-built probe (5 mm coil), equipped with a goniometer. All experiments were recorded using quadrature detection with a digitizing rate of 2 MHz and appropriate phase cycling schemes. If necessary, high-power proton decoupling ($\gamma B_2/2\pi = 34$ kHz) was employed. The number of scans varied between 32 and 2000, depending on the particular sample and type of experiment. The temperature of the samples was controlled by using a modified temperature-control unit, operating in the range $120\,K < T < 575\,K$.

A Fortran program package was employed to analyse the ^{2}H N.M.R. experiments. The programs simulate multipulse dynamic N.M.R. experiments of $I = 1$ spin systems undergoing inter- and intramolecular motion in an anisotropic medium. The corresponding numerical integrations of equation (4) are readily achieved using the Lanczos algorithm [39]. In the case of large matrix dimensions ($N \geqq 1000$) the Lanczos algorithm was found to yield reliable numerical results with considerable reduction in computing time and computer storage requirements. Within the Redfield limit [40] approximate analytical solutions [41, 42] of equation (4) are employed.

3.3. *Data analysis*

Table 2 summarizes the constant parameters used in the computations. They were obtained from an analysis of fast-rotational and slow-motion quadrupole echo spectra. As observed previously, the quadrupole coupling constants e^2qQ/h differ slightly for aromatic and aliphatic deuterons [43]. However, within the limits of error, the asymmetry parameter η is always zero.

Analysis of the ^{2}H N.M.R. experiments requires knowledge of the orientation of the various molecular tensors in the systems studied. Because of internal mobility, there are several discrete orientations for each deuteron site. The Euler angles

Table 2. Constant parameters used in the analysis of multipulse dynamic N.M.R. experiments of deuteriated model compounds and parent liquid-crystal polymers.

Deuteron spin-label site	Quadrupole coupling constant e^2qQ/h/kHz	Magnetic-tensor orientation		Molecular-frame orientation	
		θ_K/°	ψ_K/°	ϕ_M/°	θ_M/°
M1, **D1**, **P1** (a)	185	−61, −61	0, 180		−1
M1, **D1**, **P1** (b)	185	−119·2, −119·2	0, 180		−1
M1, **D1**, **P1** (c)	185	56, 56	0, 180		−1
M2, **D2**, **P2**	165	90, 90, −144·75, −35·25	144·75, 35·25, 90, 90	90	12
M3, **D3**, **P3**	165	90, 90, 144·75, 35·25	−144·75, −35·25, 90, 90	90	12
M4	55†	−144·75, 90, 90, −35·25	90, 144·75, 35·25, 90	90	12
P4 (a)	185	60, 60	0, 180	0	−12
P4 (b)	185	120·5, 120·5	0, 180	0	−12
D5, **P5** (a)	185	−61, −61	0, 180		−1
D5, **P5** (b)	185	−119·2, −119·2	0, 180		−1
D5, **P5** (c)	185	56, 56	0, 180		−1
D6, **P6**	165	90, 90, −144·75, −35·25	144·75, 35·25, 90, 90	90	12

† Motionally averaged owing to methyl-group rotation.

θ_K, ψ_K characterizing these conformations in the local molecular frame are listed in table 2.

Angular-dependent slow-motion lineshapes of the polymers **P1–P6** indicate that each repeating unit can be characterized by an order tensor axially symmetric along **Z** ($A_{20} = 0$) [4, 13]. This finding corresponds to the overall shape of the repeating unit, which is also expected to exhibit axially symmetric rotational diffusion about the Z axis. The orientation of **Z** relative to the local molecular frame is conveniently evaluated from the angular-dependent lineshapes. A schematic representation is shown in figure 1. The values for the corresponding Euler angles ϕ_M and θ_M are given in table 2. It is found that the model compounds exhibit the same molecular geometry as the polymers. Generally, molecular tilt angles from angular-dependent spectra are in good agreement with those evaluated from motionally averaged spectra at a single orientation, employing inequivalent deuterons.

The variable parameters A_{00}, n_1, n_2, n_3, n_4, $\tau_{R\perp}$, $\tau_{R\parallel}$ and τ_J were determined by computer analysis of the various ^{2}H N.M.R. experiments at any given temperature. However, they need not all be evaluated. In general, the *gauche* conformations at a particular aliphatic chain segment are equally populated, corresponding to $n_2 = n_3$. From the normalization condition, we obtain $n_2 = \frac{1}{2}(1 - n_1 - n_4)$. Consequently, there are only two unknown populations, namely n_1 and n_4.

Evaluation of the remaining parameters A_{00}, n_1, n_4, $\tau_{R\perp}$, $\tau_{R\parallel}$ and τ_J still requires a special strategy. In the fast-motion regime, the parameters of orientational order A_{00} (S_{ZZ}) [33] are conveniently obtained from the N.M.R. spectra of model compounds labelled at the mesogenic units. For a given molecular geometry, the quadrupole splitting $\Delta\nu$ of the phenyl deuterons is unambiguously related to the magnitude of S_{ZZ}. From the reduced line separation $\Delta\nu/S_{ZZ}$ of alkyl deuterons, the conformational order at the particular labelled segment can be determined. Note, however, that this reduced splitting only contains information on $n_1 - n_4$, insufficient for the evaluation of the complete order matrix [25]. Thus, except for the δ-position of the monomer, where two different spin-labels are available (**M3** and **M4**), the determination of the segmental order requires an additional N.M.R. measurement, as discussed below.

Evaluation of the dynamic parameters $\tau_{R\perp}$, $\tau_{R\parallel}$ and τ_J is achieved by employing various relaxation experiments. Since the anisotropy ratio of the intermolecular motion is practically independent of temperature, $\tau_{R\perp}/\tau_{R\parallel}$ need be determined only once for a given model compound. Generally, each experiment defines a specific dynamic window in which molecular motions can be studied [13, 25]. For instance, the spin–lattic relaxation times T_{1Z} (from inversion and saturation recovery sequences) are particularly sensitive to motions with correlation times $\tau_R \approx \omega_0^{-1}$. Thus, by employing a high magnetic field ($B_z = 7$ T), fast molecular dynamics in the range 10^{-12}–10^{-7} s can be studied. In contrast, measurement of the spin–spin relaxation time T_{2E} (from quadrupole echo sequences) permits the study of much slower motions. Since T_{2E} is most sensitive to motions with correlation times $\tau_R \approx (e^2qQ/\hbar)^{-1}$, quadrupole echo sequences offer a means to study molecular dynamics in the range 10^{-8} s $< \tau_R < 10^{-4}$ s. The analysis is completed if all relaxation experiments can be simulated using the same set of parameters. Generally, a consistent description of the overall rotational motion is obtained for all positions of labelling.

4. Results

4.1. *Lineshapes and relaxation*

Macroscopically aligned samples of the model compounds (**M1–M4**, **D1–D3**, **D5**, **D6**) and parent LCPs (**P1–P6**) [13] have been studied over a wide temperature range,

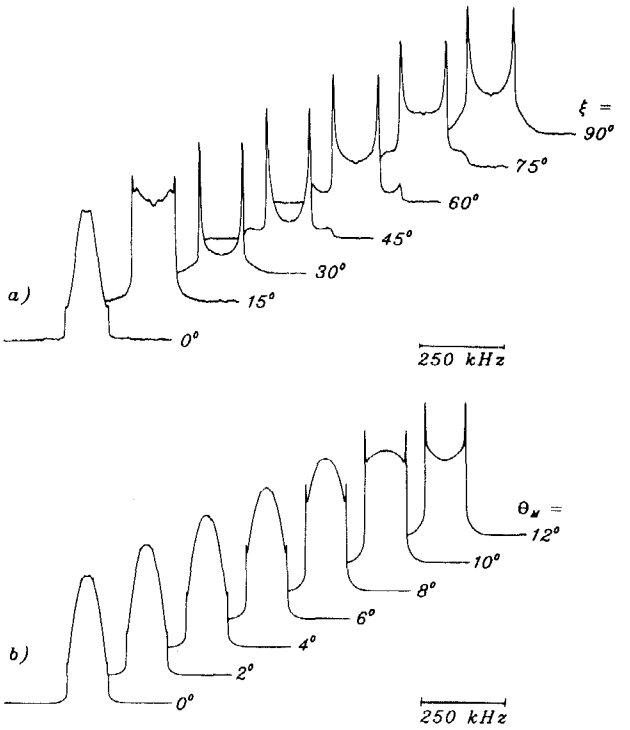

Figure 4. (*a*) Angular-dependent lineshapes of macroscopically aligned polymers **P1** at seven different orientations. ξ denotes the angle between the alignment axis and the magnetic-field direction. The spectra refer to a quadrupole echo sequence at a fixed pulse separation time of 25 μs. (*b*) Calculated ^{2}H quadrupolar echo lineshapes showing the dependence of the molecular tilt angle θ_M. The spectra are calculated using the angles (ϕ_K, θ_K, ψ_K) given in table 2, $\xi = 0°$, $\tau_J \geqq 10^{-3}$ s and $A_{00} = 9$ (equation (7)).

employing multipulse dynamic N.M.R. techniques. Representative results are shown in figures 4–10. The observed ^{2}H N.M.R. lineshapes and relaxation curves, varying dramatically with magnetic-field orientation, demonstrate the power of the method.

Figure 4(*a*) depicts the angular variation of quadrupole echo lineshapes at $T = 253$ K. The spectra refer to the polymer **P1** and seven different orientations ξ of alignment axis and magnetic field. Very large spectral changes are observed when the sample is rotated, showing that liquid-crystalline order is maintained in the solid and glassy states of the polymer. The pronounced angular dependence of the spectra was employed to evaluate the molecular geometry of the systems. Figure 4(*b*) shows calculated lineshapes for $\xi = 0°$ and different values of the tilt angle θ_M, characterizing the orientation of the order tensor relative to the central phenyl ring (figure 1). Apparently, the tilt angle is close to zero in this case (table 2).

Figure 5 compares fast-rotational spectra of monomers (**M1–M4**, figures 5(*a*)–(*d*)) and dimers (**D1–D3**, figures 5(*e*)–(*g*)), demonstrating the effect of the molecular weight on the spectral feature. The lineshapes refer to the same reduced temperature ($T/T_{ni} = 0{\cdot}88$) and parallel orientation of alignment axis and magnetic field. Note that systems labelled at the central phenyl ring (**M1** and **D1**, figures 5(*a*, *e*)) exhibit three different quadrupole splittings, owing to the presence of inequivalent deuterons. The inequivalence is due to different orientations of the various C–D

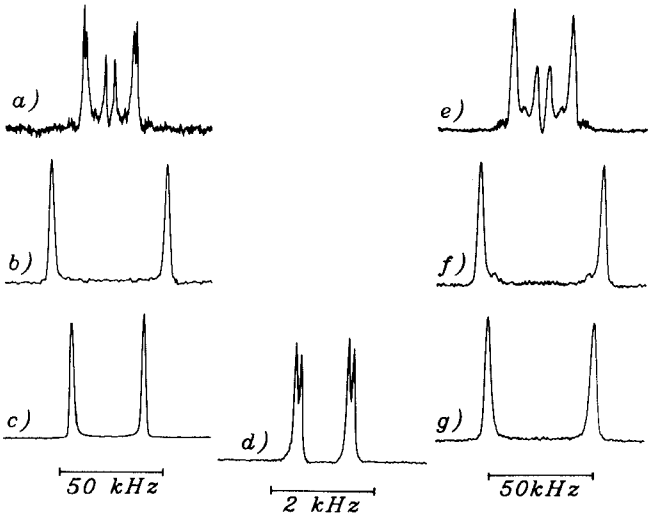

Figure 5. Experimental ^2H quadrupolar echo spectra of specifically deuteriated model compounds in the nematic phase. The lineshapes are recorded for the same reduced temperature ($T^* = T/T_{ni} = 0{\cdot}88$) and parallel orientation of nematic director and magnetic field, i.e. $\xi = 0°$, and refer to (*a*) **M1**, (*b*) **M2**, (*c*) **M3**, (*d*) **M4**, (*e*) **D1**, (*f*) **D2**, (*g*) **D3**. Note that that spectrum (*d*) is drawn on a different scale.

bonds relative to the para-axis of the phenyl ring (table 2). In contrast, the N.M.R. spectra of model compounds deuteriated in the alkyl groups show a single splitting. A comparison of the spectra of monomers (figures 5 (*a*)–(*c*)) and corresponding dimers (figures 5 (*e*)–(*g*)) reveals a consistent larger splitting for the latter compounds. Evidently, molecular order of the model compounds also depends on the degree of polymerization.

An unexpected lineshape is observed for the monomer **M4**, labelled at the terminal methyl groups (figure 5 (*d*)). Here two different splittings are resolved upon proton decoupling, indicating a slight distortion from the expected C_2 symmetry of the molecule [44, 45]. Since this additional splitting is only 200 Hz and independent of temperature, we shall ignore it in the analysis, assuming the same average tilt angle θ_M for both alkyl tails (table 2).

In figure 6 the spin–lattice relaxation times T_{1Z} of various model compounds are plotted as a function of $1/T$. All relaxation times refer to parallel orientation of alignment axis and magnetic field. Full symbols denote monomers (**M2–M4**) while open symbols characterize dimers (**D2, D3**). The various label positions are distinguished by circles (α-segment), squares (δ-segment) and triangles (ε-segment) respectively. We see that the temperature dependences in the nematic phase are quite similar. For all systems, the T_{1Z} curves decrease with decreasing temperature. However, the Arrhenius plots are generally non-linear, indicating that different motional modes contribute to spin–lattice relaxation of the model compounds.

The observed lineshapes and relaxation curves were simulated, employing the N.M.R. model outlined above. An iterative fit of several pulse-dependent experiments for any given temperature provided reliable values for the simulation parameters, i.e. the rotational correlation times and the parameters of orientational and conformational order. The solid lines in figure 6 represent best-fit simulations. They agree favourably with their experimental counterparts. Note that relaxation curves for three

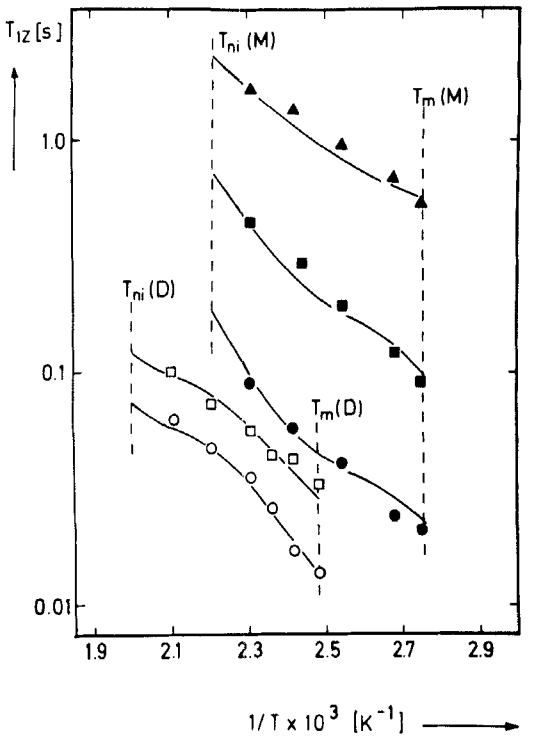

Figure 6. Arrhenius representation of ^2H spin–lattice relaxation times T_{1Z} of model compounds deuteriated at different positions in the alkyl chains. Filled symbols denote the monomers, while open symbols refer to the dimers with ten methylene units in the aliphatic spacer, i.e. **D2** and **D3**. The various positions of the deuteron spin-labels are represented by circles (α-position; **D2**, **M2**), squares (δ-position; **D3**, **M3**) and triangles (ε-position, **M4**). Dashed lines indicate different phase transitions.

different label positions are reproduced by our model with the same set of simulation parameters. In the following we describe the results in more detail, treating the various simulation parameters separately.

4.2. *Order parameters*

Molecular order of the model compounds and parent LCPs comprises the conformational order of the alkyl chains and the orientational order of the mesogenic units. Conformational order in these systems is conveniently described in terms of segmental order parameters $S_{Z'Z'}$ and $S_{X'X'} - S_{Y'Y'}$, defined elsewhere [25]. Within the limits of a completely disordered segment, all four tetrahedron sites are equally populated, resulting in an order parameter $S_{Z'Z'} = 0$. At the other extreme, a fully extended chain is fixed to its all-*trans* conformation, and the order parameter $S_{Z'Z'}$ becomes equal to unity.

In figure 7 these order parameters are plotted as functions of the reduced temperature $T^* = T/T_{ni}$. They refer to the monomers **M2**–**M4** (triangles), dimers **D2**, **D3** (squares) and polymers **P2**, **P3** (circles) respectively. The α- and δ-segments are distinguished by open and filled symbols. Generally, the maximum error for the given $S_{Z'Z'}$ values is ±4 per cent.

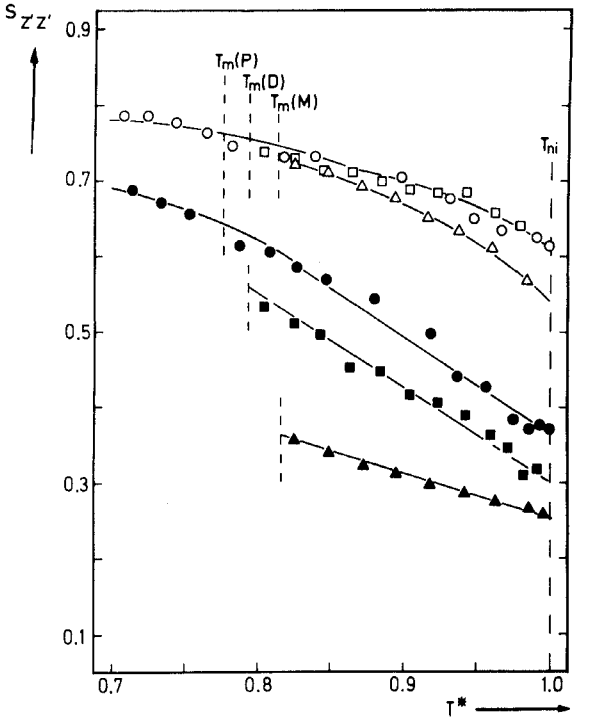

Figure 7. Temperature dependence of conformational order of model compounds and parent liquid-crystal polymers, expressed in terms of segmental order parameters $S_{Z'Z'}$ at various chain segments. $S_{Z'Z'}$ characterizes the ordering of the most-ordered segmental axis with respect to the chain axis. Open symbols refer to the α-positions, while filled symbols denote the δ-positions. The different compounds are denoted by circles (polymers with ten methylene units in the flexible spacer), squares (dimers with ten methylene units in the flexible spacer) and triangles (monomers). Dashed lines indicate different phase transitions.

At the isotropic–nematic transition ($T^* = 1{\cdot}0$) order parameters with values between $S_{Z'Z'} = 0{\cdot}61$ and $S_{Z'Z'} = 0{\cdot}25$ are observed. Note, however, that conformational order of the α-segment ($0{\cdot}56 \leqq S_{Z'Z'} \leqq 0{\cdot}61$) is nearly independent of the degree of polymerization. This applies also to the dimers/polymers having only nine spacer segments (**D6/P6**). In contrast, for the δ-position a systematic increase in $S_{Z'Z'}$ from $S_{Z'Z'} = 0{\cdot}25$ (monomers) via $S_{Z'Z'} = 0{\cdot}30$ (dimers) to $S_{Z'Z'} = 0{\cdot}37$ (polymers) is detected. No such comprehensive data for systems with nine spacer segments are yet available.

Lowering the temperature increases the conformational order at all positions. Note, however, that the central units of the *spacer* (dimers and polymers) order faster than the outer ones. Thus at lower temperatures a uniform segmental order for all spacer segments is expected and actually observed [10, 13, 15]. In contrast, the segmental order parameters of the *pendent groups* (monomers) diverge with decreasing temperature. Generally, the anisotropy of the segmental order is small for all systems, varying between $0{\cdot}11 \leqq S_{X'X'} - S_{Y'Y'} \leqq 0{\cdot}18$ (not shown).

Orientational order is described in terms of the conventional order parameter S_{ZZ}, characterizing the average orientation of the molecular Z axis (figure 1) with respect to the director [46]. In figure 8 the order parameters S_{ZZ} of the various systems are

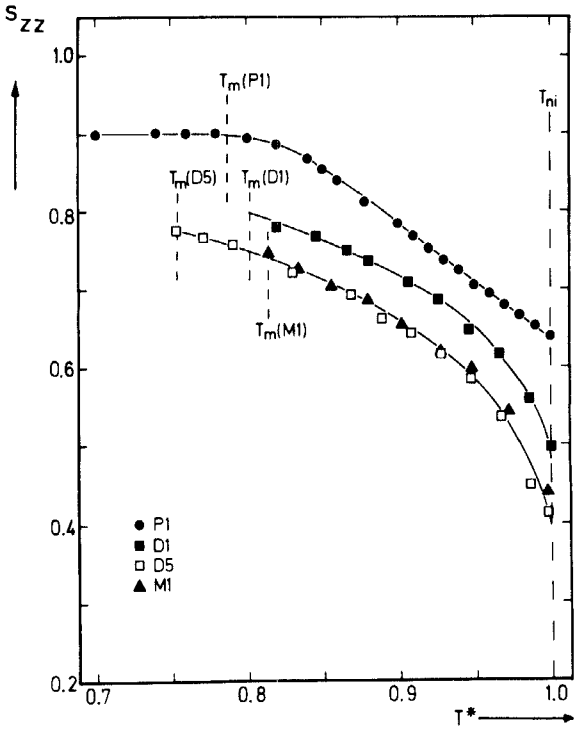

Figure 8. Temperature dependence of the orientational order in the nematic phase of model compounds and parent liquid-crystal polymers, expressed by the conventional order parameter S_{ZZ}, characterizing the average orientation of the long molecular axes with respect to the director. Filled circles denote polymers **P1**, squares refer to the dimers with ten (full symbols) and with nine (open symbols) methylene units in the aliphatic spacer. The monomers are represented by filled triangles. Dashed lines indicate different phase transitions.

plotted as functions of the reduced temperature $T^* = T/T_{ni}$. Triangles refer to monomers, filled (ten spacer segments) and open squares (nine spacer segments) denote dimers, while circles correspond to the polymers (ten spacer segments). The uncertainty in S_{ZZ} is generally less than 4 per cent.

In the isotropic phase all order parameters are $S_{ZZ} = 0$, indicating a random orientation of the molecules. At the isotropic–nematic transition ($T^* = 1{\cdot}0$) the order parameters jump to finite values, which depend on the degree of polymerization and parity of the spacer. In the case of ten methylene segments a stepwise increase from the monomers ($S_{ZZ} = 0{\cdot}43$) via the dimers ($S_{ZZ} = 0{\cdot}50$) to the polymers ($S_{ZZ} = 0{\cdot}64$) is observed. Note that dimers with nine spacer segments exhibit the lower order parameter ($S_{ZZ} = 0{\cdot}42$) of the monomers.

Lowering the temperature increases S_{ZZ} for all nematogens, maintaining the gradual differences at T^*. Interestingly, orientational order of the polymers is quantitatively retained in the solid and glassy states of the systems. No change of $S_{ZZ} = 0{\cdot}90$ is observed after keeping the sample at room temperature. In contrast, liquid-crystalline order of the model compounds is completely lost upon crystallization.

4.3. *Motional correlation times*

In figures 9 and 10 the correlation times for various motions of the nematogens are plotted as functions of $1/T$. They refer to the monomers **M1–M4** (triangles), dimers **D1–D3** (squares) and polymers **P1–P3** (circles). Inspection of the logarithmic plots reveals a large dynamic range, extending over six orders of magnitude. The uncertainty in correlation times is generally < 10 per cent, except for *trans–gauche* isomerization at the δ-position, which has only a marginal effect on T_{1Z} relaxation at 46 MHz.

We see that the Arrhenius plots are generally linear within the nematic phase, and activation energies for the various motions have been determined from the slopes of the straight lines. They are listed in table 3. The activation energies for *trans–gauche* isomerization of $15{\cdot}2\,\text{kJ/mol} \leqq E_J \leqq 16{\cdot}3\,\text{kJ/mol}$ correspond to the local character of this motion. Higher activation energies of $39{\cdot}9\,\text{kJ/mol} \leqq E_{R\|} \leqq 48{\cdot}3\,\text{kJ/mol}$ are observed for long-axis rotation, representing reorientations of the molecules as a whole. Strictly, however, the Arrhenius plot for overall dynamics of the polymers is non-linear, the apparent activation energy increasing with decreasing temperature [13, 15].

The squares and triangles in figure 9 indicate correlation times for *trans-gauche* isomerization in model compounds. We see that these motions are considerably rapid,

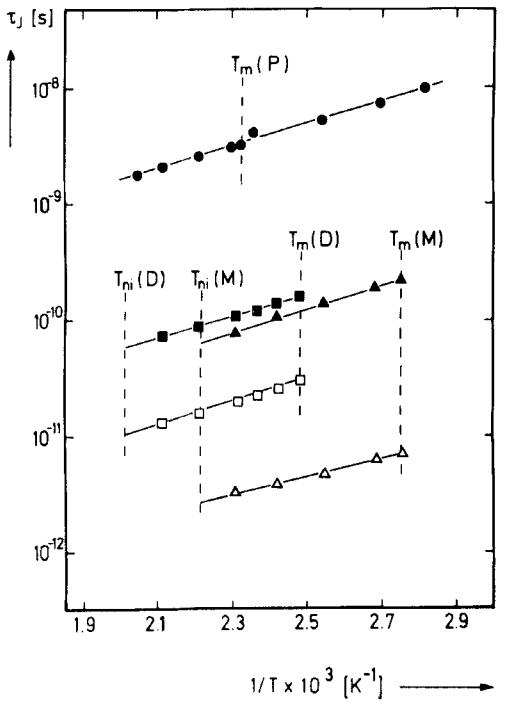

Figure 9. Arrhenius representation of various correlation times τ_J, characterizing the intramolecular dynamics of labelled methylene units in the alkyl chains of the semiflexible molecules. Filled symbols denote the α-positions, while open symbols refer to the δ-positions. The various compounds are denoted by triangles (monomers), squares (dimers) and circles (polymers). Only compounds with ten methylene units in the flexible spacer (dimers, polymers) are shown. Dashed lines indicate different phase transitions.

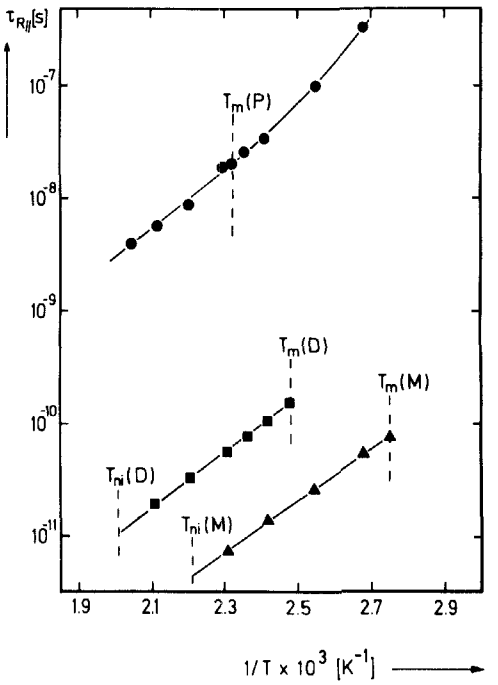

Figure 10. Arrhenius representation of the intermolecular correlation times $\tau_{R\parallel}$ of model compounds and parent liquid-crystal polymers in the nematic phase. Triangles refer to monomers, squares correspond to the dimers and circles denote the polymers. Only compounds with ten methylene units in the aliphatic spacer (dimers, polymers) are shown. The activation energies taken from the slopes are 39·9 kJ/mol (monomers), 46·1 kJ/mol (dimers) and 48·3 kJ/mol (polymers). Dashed lines indicate different phase transitions.

Table 3. Activation energies of molecular motions, characterizing the nematic phase of the model compounds and parent liquid-crystal polymers.

Liquid-crystal system	Activation energies			Anisotropy ratio
	$E_{R\parallel}$/kJ mol^{-1}	$E_J(\alpha$ – C)/kJ mol^{-1}	$E_J(\delta$ – C)/kJ mol^{-1}	$\tau_{R\perp}/\tau_{R\parallel}$
M1–M4	39·9	16·1	15·3	8
D1–D3	46·1	16·3	15·2	25
P1–P4	48·3	15·9		11

exhibiting correlation times of 10^{-12} s $< \tau_J < 10^{-10}$ s. Consequently, their effect on T_{1Z} is rather small. Note the pronounced mobility gradient along the aliphatic chains. Apparently, the rate of *trans–gauche* isomerization increases considerably from the α- to the δ-segment.

Figure 10 compares the rates for intermolecular motion of model compounds and parent LCPs. Generally, the correlation times for overall rotation are found to be several orders of magnitude faster in the former case. Within the nematic range, long-axis rotation of the model compounds occurs with correlation times of 10^{-11} s $< \tau_{R\parallel} < 10^{-10}$ s. The evaluated anisotropy ratios of $\tau_{R\perp}/\tau_{R\parallel} = 8$ (monomers) and $\tau_{R\perp}/\tau_{R\parallel} = 25$ (dimers) correspond to the dimensions of the molecules [47]. Note that

this detailed information about molecular motion could be obtained only by employing multipulse dynamic N.M.R. techniques.

5. Discussion

Our present knowledge about the molecular properties of model compounds, derived from semiflexible LCPs, originates to a large extent from N.M.R. studies using ^1H and ^2H nuclei. These investigations provided information about the dynamic organization of the model compounds comprising orientational and conformational order in the various mesophases [21–24]. For a complete molecular characterization, however, N.M.R. relaxation studies are required. The use of a comprehensive relaxation model offers the chance to detect the various motions unambiguously [13, 25]. In addition, molecular order and geometry can be determined.

5.1. *Molecular geometry*

The parameters characterizing the geometry of the model compounds and parent LCPs are summarized in table 2. They were obtained from an analysis of site- and angular-dependent ^2H N.M.R. spectra. Generally, the given bond and tilt angles are in good agreement with literature values [48–52], and thus provide a consistent description of the molecular structure. In particular, the evaluated coplanar arrangement of outer phenyl ring and adjacent *O*-alkyl group corresponds to previous findings [48, 49, 51, 52]. Note that the torsional angle ϕ_M of the central phenyl ring, estimated as $\phi_M \approx 65°$ [50], is not determined by our experiments, since the *p*-axis accidentally coincides with the symmetry axis of the order tensor (figure 1).

5.2. *Molecular order*

Molecular order of the semiflexible molecules is specified by three different order parameters: S_{ZZ}, $S_{Z'Z'}(\alpha\text{-C})$, and $S_{Z'Z'}(\delta\text{-C})$. They refer to the orientational order of the mesogenic units and the conformational order at the α- and δ-segments respectively. In figure 7 the latter order parameters are plotted as functions of the reduced temperature T^*.

For the α-methylene groups, adjacent to the mesogenic units, a high degree of conformational order is observed, practically independent of the molecular weight of the systems. Note that the minor differences in conformational order between monomer, dimer and polymer at T_{ni} completely vanish at the melt transitions. The observed high $S_{Z'Z'}$ values for the α-segments can be rationalized by the close vicinity of the mesogenic cores.

For the δ-segments the dependence of the conformational order on the specific molecular structure is much more pronounced. At the clearing point T_{ni} we observe a stepwise increase of $S_{Z'Z'}$ from the monomer via the dimer to the polymer. Note, however, that all $S_{Z'Z'}$ values at the δ-position are significantly smaller than those evaluated for the α-segments. Apparently, there is an order gradient along the chains, which varies from system to system studied.

Decreasing the temperature increases conformational order at all positions. In the case of the monomers, however, the increase at the δ-segment is smaller than the corresponding increase at the α-segment, leading to an enhanced order gradient at lower temperatures. In contrast, the segmental order parameters of the dimers and polymers converge upon cooling, resulting in a reduced order gradient. Thus,

ultimately, a uniform segmental order for all spacer segments is expected, and is actually observed for the polymers [10, 13, 15]. One should note the distinctive behaviour of the aliphatic chains in the *spacer* groups of the dimers and polymers and in the terminal *pendent* groups of the monomers.

As mentioned above, there is an order or 'flexibility' gradient along the aliphatic chains. Table 4 summarizes the results for the model compounds and parent LCPs. Note that the populations n_1–n_4 of all conformational states [32], accessible at a particular segment, are presented. Apparently, the segmental order parameter $S_{Z'Z'}$, evaluated from the populations n_i, significantly decreases from the α- to the δ-positions. Interestingly, the anisotropy of the segmental order $S_{X'X'} - S_{Y'Y'}$ remains constant for the various positions. Interpretation of these chain-ordering data in terms of statistical-mechanical models of liquid crystals presents a challenging theoretical problem [16, 53, 54].

Table 4. Conformational order of the model compounds and parent liquid-crystal polymers, characterizing the order gradient in the nematic phase ($T^* = 0{\cdot}85$).

Liquid-crystal system	Chain segment	Populations of the conformational states				Segmental order parameters		Orientational order parameter
		n_1	n_2	n_3	n_4	$S_{Z'Z'}$	$S_{X'X'} - S_{Y'Y'}$	S_{ZZ}
M1–M4	α-C	0·78	0·10	0·10	0·02	0·71	0·11	0·71
M1–M4	δ-C	0·50	0·20	0·20	0·10	0·34	0·14	0·71
D1–D3	α-C	0·78	0·11	0·11	0·00	0·71	0·15	0·76
D1–D3	δ-C	0·62	0·17	0·17	0·04	0·50	0·18	0·76
P1–P4	α-C	0·78	0·11	0·11	0·00	0·71	0·15	0·85
P1–P4	δ-C	0·68	0·14	0·14	0·04	0·58	0·14	0·85

Inspection of figure 7 reveals that the dimers **D1–D3** are 'good' model compounds for the corresponding polymers **P1–P4**. However, the appropriate model systems have to be chosen carefully. In a recent N.M.R. investigation of related dimers ($H_{21}C_{10}$-O-Φ-COO-Φ-O-$(CD_2)_{10}$-O-Φ-OOC-Φ-O-$C_{10}H_{21}$) a divergence of $S_{Z'Z'}$ with decreasing temperature was observed [24]. This result, which is at variance with the present finding, can be rationalized in terms of an unfavourable packing of the molecules in the nematic phase, due to incommensurable pendent groups. Interestingly, shortening of the pendent alkyl chains to five methylene units leads to model systems with converging segmental order parameters at lower temperatures [55].

The observed $S_{Z'Z'}$ values for the dimers **D1–D3** and polymers **P1–P4** imply rather high *trans* populations throughout the spacer. Evidently, highly extended conformers prevail in the nematic phase of these systems. This finding is the most prominent feature distinguishing liquid-crystalline main-chain polymers from side-chain polymers [56, 57] and their monomeric analogues [53, 54, 58]. Predictions of statistical-mechanical theories [3, 14, 16] are in qualitative agreement with the N.M.R. results. It appears that a number of unique properties exhibited by main-chain polymers can be attributed to the conformational order, which is restricted to highly extended configurations [14].

We now discuss the orientational order of the model compounds and parent LCPs in terms of the familiar order parameter S_{ZZ}, characterizing the average orientation of the molecular Z axis with respect to the nematic director [46]. In figure 8 these order parameters are plotted as a function of the reduced temperature T^*.

Let us first discuss the order parameters of systems having ten methylene segments in the repeating unit ('even-numbered' systems). At the isotropic–nematic transition all order parameters jump to finite values, showing a stepwise increase from $S_{ZZ} = 0{\cdot}43$ (monomers) to $S_{ZZ} = 0{\cdot}50$ (dimers) and $S_{ZZ} = 0{\cdot}64$ (polymers). This dependence of orientational order on the degree of polymerization is reflected by the transition entropies ΔS_{ni} (table 1), which vary between $\Delta S_{ni} = 4{\cdot}6\,J/(mol\,K)$, $\Delta S_{ni} = 8{\cdot}0\,J/(mol\,K)$ and $\Delta S_{ni} = 12{\cdot}1\,J/(mol\,K)$. Similar thermodynamic data have been reported for other model compounds and parent LCPs [17–21].

Lowering the temperature increases S_{ZZ} for all nematogens to limiting values of $S_{ZZ} = 0{\cdot}75$ (monomers), $S_{ZZ} = 0{\cdot}80$ (dimers) and $S_{ZZ} = 0{\cdot}90$ (polymers) at the corresponding melt transitions. Note that the orientational order of the polymers **P1–P4** considerably exceeds that exhibited by side-chain polymers [56, 57] and low-molecular-weight nematogens [53, 54, 58]. As predicted [2, 3, 14], the polymer chains are highly ordered on a molecular level, in agreement with E.S.R. [7] and ^1H N.M.R. studies [11].

The pronounced increase in S_{ZZ} from the monomers to the dimers agrees with previous findings [6, 22, 23]. Within experimental error, the S_{ZZ} values of the dimers correspond to the mean order parameters of the monomers and polymers, consistent with theoretical predictions [14]. The observed abrupt increase in molecular order is apparently caused by intramolecular order transfer via highly extended spacers. Consequently, linking of additional mesogenic units by flexible spacers should further increase the orientational order of the systems. Recent investigations on trimeric and tetrameric model compounds support these considerations [59, 60].

So far, the discussion has referred to systems having ten segments in the repeating unit. Reducing the alkyl chain length to nine methylene groups ('odd-numbered' systems) causes a pronounced change in the order parameter S_{ZZ}. The results for the dimers **D5** and **D6**, denoted by open squares (figure 8), indicate a significant reduction in S_{ZZ} in the nematic phase. Note that the 'odd-numbered' dimers only exhibit the lower order parameters of the monomers. This pronounced even–odd effect—also observed for other dimeric [22, 23] and polymeric liquid crystals [8, 13, 15]—presents an interesting theoretical problem. Statistical-mechanical treatments of this phenomenon have recently appeared [3, 14, 16]. They are in substantial agreement with the present N.M.R. results.

Orientational order of liquid crystals in bulk samples comprises the orientational order of the molecules with respect to the local director and the macroscopic alignment of the director axes in the laboratory frame (macroorder). The latter order is conveniently described in terms of a macro-order parameter $S_{z''z''}$ defined elsewhere [4, 13, 56]. For a random distribution of director axes $S_{z''z''} = 0$. In the case of complete alignment we expect $S_{z''z''} = 1{\cdot}0$ or $S_{z''z''} = -0{\cdot}5$, depending on the sign of the dielectric/diamagnetic anisotropy of the system.

Experimental values of $S_{z''z''}$ for the model compounds and parent LCPs **M1–P3** were obtained, employing dynamic E.S.R. techniques [61]. Since the dielectric anisotropy of all systems is negative, only a two-dimensional distribution of director axes ($S_{z''z''} = -0{\cdot}5$) can be achieved using high electric fields. However, a uniform alignment of the domains ($S_{z''z''} = 1{\cdot}0$) is obtained by strong magnetic fields. The required field strengths B depend critically on the degree of polymerization. For the monomers **M1–M3** complete alignment is achieved at $B = 0{\cdot}33\,T$, whereas for the dimers **D1–D3** a field of $B = 0{\cdot}7\,T$ is required. The corresponding field strengths of the polymers **P1–P4** exceed these values by a considerable amount. As reported previously

[13], no alignment is achieved for $B = 1{\cdot}5\,T$, whereas complete macroscopic orientation is achieved at $B = 7\,T$. It has been shown that field-induced director reorientation occurs only above a threshold field B_c, which is directly related to the effective elastic constant k_i of the system [62, 63]. Preliminary N.M.R. studies of the polymers **P1–P4** yield elastic constants that exceed those of the corresponding model compounds by two orders of magnitude, in agreement with recent studies on other LCPs [56, 64].

Interestingly, orientational order of the polymers is quantitatively retained when the sample is cooled below the melting point and glass transition [13]. No change in S_{ZZ} is observed, even on keeping the sample at room temperature. Thus, in contrast with the model compounds, long-range orientational order is preserved even upon crystallization. This particular behaviour of LCPs provides the basis for their excellent mechanical properties [65, 66]. For example, melt spinning of the polymers **P1–P4** produces highly oriented fibres with tensile moduli up to $E = 22\,GPa$ [4]. Analysis of angular-dependent N.M.R. experiments, performed on the solid fibres, yielded an orientational order parameter of $S_{ZZ} = 0{\cdot}9$, with practically all of the domains aligned in draw direction, $S_{z''z''} > 0{\cdot}95$. High modulus and strength ($T = 0{\cdot}34\,GPa$) result from this highly oriented chain configuration, maintained in the solid state of the polymer [4].

In contrast, long-range orientational order of the model compounds **M1–D3** is completely lost upon crystallization. Thus, despite the fact that dimers already achieve rather high order parameters in the nematic phase, many of the exceptional properties of LCPs are restricted to systems with higher molecular weights. In this respect, oligomers with defined molar masses are presently being studied [60].

5.3. *Molecular dynamics*

The molecular dynamics of the model compounds and parent LCPs is specified in terms of the correlation times $\tau_{R\parallel}$, $\tau_{R\perp}$, $\tau_J(\alpha\text{-C})$ and $\tau_J(\delta\text{-C})$. They refer to overall rotation about the diffusion-tensor axis Z, reorientation of this axis, and *trans–gauche* isomerization at the α- and δ-segments respectively. Logarithmic plots of these correlation times versus $1/T$ give straight lines (figures 9 and 10). From the Arrhenius plots, we obtain the activation energies of the various motions, listed in table 3.

In the nematic phase the correlation times for *trans–gauche* isomerization range from 10^{-12} s (monomer, δ-segment) to 10^{-9} s (polymer, α-segment). Note the distinct rate of conformational reorientation at comparable sites of the various systems. Apparently, *trans–gauche* isomerization in the polymers is at least one order of magnitude slower than in the model compounds. The average activation energy for this process of $E_J = 15{\cdot}8\,kJ/mol$ can be compared with the potential-barrier height encountered in rotational isomerization about C–C bonds [32].

Inspection of figure 9 reveals a pronounced dependence of the *trans–gauche* isomerization rate on the label position, increasing considerably from the α- to the δ-segment. Evidently, there is a significant mobility gradient along the alkyl chains. Note that τ_J in the *pendent groups* of the monomers decreases by two orders of magnitude from the α- to the δ-position, in qualitative agreement with theoretical predictions [67]. On the other hand, a much less pronounced mobility gradient is observed for the *spacers* of the dimers and polymers [60], presumably because of the increased conformational order in these systems.

The correlation times $7 \times 10^{-12}\,s < \tau_{R\parallel} < 1{\cdot}5 \times 10^{-10}\,s$ for overall rotation of the model compounds in the nematic phase (figure 10) correspond to those reported

for other low-molar-mass systems [68–72]. In addition, the evaluated anisotropy ratios $\tau_{R\perp}/\tau_{R\parallel} = 8$ (monomers) and $\tau_{R\perp}/\tau_{R\parallel} = 25$ (dimers) are in excellent agreement with the theoretical values of 8·7 and 26·5, calculated from the corresponding molecular dimensions [47]. The fact that a consistent description of the overall molecular motion can be obtained for all positions of labelling supports the motional model. It further demonstrates the ability to discriminate between the motional modes by simulation of angular- and temperature-dependent relaxation experiments [13]. The temperature dependence yields activation energies of $39{\cdot}9\,\text{kJ/mol} < E_{R\parallel} < 48{\cdot}3\,\text{kJ/mol}$ (table 3), which clearly distinguish the intramolecular from the intermolecular motion. The segmental motion has activation energies that are comparable to the barrier height for *trans–gauche* isomerism [32], whereas the activation energies for overall motion are two to three times greater.

It is interesting to note, that with respect to dynamic properties, dimers behave like conventional monomeric liquid crystals, exhibiting much faster motions than the polymers. For example, overall rotation of the LCPs **P1–P4** occurs with correlation times of $10^{-9}\,\text{s} < \tau_{R\parallel} < 10^{-8}\,\text{s}$, in agreement with previous E.S.R. studies on liquid-crystalline main-chain [7] and side-chain polymers [56]. The two orders of magnitude in rotational rates are reflected in the bulk viscosities of the polymers, exceeding those of the monomers by nearly a factor of 1000 [61].

Molecular motions in liquid crystals may occur as isolated or collective modes. For the latter mechanism, known as order director fluctuations, a continuous distribution of correlation times is expected [71]. Recent proton T_{1Z} dispersion measurements of the model compounds and parent LCPs, carried out over a frequency range of five orders of magnitude ($10^3\,\text{Hz} < \omega_0/2\pi < 3 \times 10^6\,\text{Hz}$), clearly show that collective order fluctuations contribute to the relaxation process only at extremely low frequencies in the kHz regime, whereas the conventional MHz range is dominated by reorientations of individual molecules [73].

For nematic liquid crystals, theory predicts a characteristic dispersion law $T_{1Z}(\omega_0) \propto \omega_0^{1/2}$. This is exactly what we observe for the monomeric and dimeric systems. Although a somewhat higher exponent is evaluated for the polymers, there is no doubt that collective order fluctuations occur in these systems, likewise. The low-frequency dispersion step can only be observed for the nematic phase, but is completely absent for the solid and glassy states of the polymers, as expected [73].

6. Conclusions

Multipulse dynamic N.M.R. of model compounds, derived from thermotropic LCPs, has provided detailed information about the dynamic organization of these systems. From the dynamic point of view, the primary result is the detection and characterization of the dominant motions in liquid crystals, ranging from $10^{-12}\,\text{s}$ for internal reorientations to $10^{-3}\,\text{s}$ for director order fluctuations. Generally, dimers exhibit motional correlation times similar to conventional monomeric liquid crystals, whereas the dynamics of the polymers is considerably slower. The two-orders-of-magnitude difference in motional rates is reflected in the bulk viscosities of the polymers, which exceed those of the monomers accordingly.

New information about the molecular organization of the model compounds has been obtained. The significant increase in molecular order from the monomers to the dimers is apparently caused by intramolecular order transfer via highly extended spacers. On the other hand, long-range orientational order of the model compounds

is completely lost upon crystallization. Thus many of the exceptional mechanical properties of LCPs are restricted to systems with higher molecular weights. A prerequisite for any specific application is precise knowledge of their liquid-crystalline properties at a molecular level—something that is now obtainable using dynamic N.M.R. techniques.

It is a pleasure to thank Mrs H. Seidel for help in preparing the specifically deuteriated compounds. The authors are also grateful to Dr E. Ohmes for assistance in the numerical computations. Financial support of this work by the Deutsche Forschungsgemeinschaft and Fonds der Chemischen Industrie is gratefully acknowledged.

References

[1] FLORY, P. J., 1982, *Proc. natn. Acad. Sci. U.S.A.*, **79**, 4510.
[2] RONCA, G., and YOON, D. Y., 1982, *J. chem. Phys.*, **76**, 3295.
[3] ABE, A., 1984, *Macromolecules*, **17**, 2280.
[4] MÜLLER, K., SCHLEICHER, A., OHMES, E., FERRARINI, A., and KOTHE, G., 1987, *Macromolecules*, **20**, 2761.
[5] LIEBERT, L., STRZELECKI, L., VAN LUYEN, D., and LEVELUT, A. M., 1981, *Eur. Polym. J.*, **17**, 71.
[6] SIGAUD, G., YOON, D. Y., and GRIFFIN, A. C., 1983, *Macromolecules*, **16**, 875.
[7] MÜLLER, K., WASSMER, K.-H., LENZ, R. W., and KOTHE, G., 1983, *J. Polym. Sci. Polym. Lett. Ed.*, **21**, 785.
[8] MARTINS, A. F., FERREIRA, J. B., VOLINO, F., BLUMSTEIN, A., and BLUMSTEIN, R. B., 1983, *Macromolecules*, **16**, 279.
[9] SAMULSKI, E. T., GAUTHIER, M. M., BLUMSTEIN, R. B., and BLUMSTEIN, A., 1984, *Macromolecules*, **17**, 479.
[10] MÜLLER, K., HISGEN, B., RINGSDORF, H., LENZ, R. W., and KOTHE, G., 1984, *Molec. Crystals liq. Crystals*, **113**, 167.
[11] BLUMSTEIN, R. B., STICKLESS, E. M., GAUTHIER, M. M., BLUMSTEIN, A., and VOLINO, F., 1984, *Macromolecules*, **17**, 177.
[12] BRUCKNER, S., CAMPBELL SCOTT, J., YOON, D. Y., and GRIFFIN, A. C., 1985, *Macromolecules*, **18**, 2709.
[13] MÜLLER, K., MEIER, P., and KOTHE, G., 1985, *Prog. nucl. magn. Reson. Spectrosc.*, **17**, 211.
[14] YOON, D. Y., and BRUCKNER, S., 1985, *Macromolecules*, **18**, 651.
[15] MÜLLER, K., and KOTHE, G., 1985, *Ber. Bunsenges. phys. Chem.*, **89**, 1214.
[16] LUCKHURST, G. R., 1984, *Recent Advances in Liquid Crystalline Polymers*, edited by L. L. Chapoy (Elsevier), p. 105.
[17] GRIFFIN, A. C., and BRITT, T. R., 1981, *J. Am. chem. Soc.*, **103**, 4957.
[18] BLUMSTEIN, R. B., and STICKLESS, A. M., 1982, *Molec. Crystals liq. Crystals Lett.*, **82**, 151.
[19] GRIFFIN, A. C., and BRITT, T. R., 1983, *Molec. Crystals liq. Crystals Lett.*, **92**, 149.
[20] BUGLIONE, J. A., ROVIELLO, A., and SIRIGU, A., 1984, *Molec. Crystals liq. Crystals*, **106**, 169.
[21] EMSLEY, J. W., LUCKHURST, G. R., SHILSTONE, G. N., and SAGE, I., 1984, *Molec. Crystals liq. Crystals Lett.*, **102**, 223.
[22] EMSLEY, J. W., LUCKHURST, G. R., and SHILSTONE, G. N., 1984, *Molec. Phys.*, **53**, 1023.
[23] BLUMSTEIN, R. B., POLLICKS, M. D., STICKLESS, E. M., BLUMSTEIN, A., and VOLINO, F., 1985, *Molec. Crystals liq. Crystals*, **129**, 375.
[24] GRIFFIN, A. C., and SAMULSKI, E. T., 1985, *J. am. chem. Soc.*, **107**, 2975.
[25] MEIER, P., OHMES, E., and KOTHE, G., 1986, *J. chem. Phys.*, **85**, 3598.
[26] KUBO, R., 1969, *Stochastic Processes in Chemical Physics. Advances in Chemical Physics*, Vol. 15, edited by K. Shuler (Wiley), p. 101.
[27] FREED, J. H., BRUNO, G. V., and POLNASZEK, C. F., 1971, *J. phys. Chem.*, **75**, 3385.
[28] NORRIS, J. R., and WEISSMAN, S. I., 1969, *J. phys. Chem.*, **73**, 3119.
[29] KOTHE, G., 1977, *Molec. Phys.*, **33**, 147.
[30] SILLESCU, H., 1971, *J. chem. Phys.*, **54**, 2110.

[31] KOTHE, G., WASSMER, K.-H., NAUJOK, A., OHMES, E., RIESER, J., and WALLENFELS, K., 1979, *J. magn. Reson.*, **36**, 425.
[32] FLORY, P. J., 1969, *Statistical Mechanics of Chain Molecules* (Interscience).
[33] STRALEY, J. P., 1974, *Phys. Rev.* A, **10**, 1881.
[34] JIN, J.-I., ANTOUN, S., OBER, C., and LENZ, R. W., 1980, *Br. Polym. J.*, **12**, 132.
[35] ANTOUN, S., LENZ, R. W., and JIN, J.-I., 1981, *J. Polym. Sci. Polym. Chem. Ed.*, **19**, 1901.
[36] MÜLLER, K., 1985, Ph.D. Thesis, University of Stuttgart.
[37] KOHLHAMMER, K., 1985, Diploma Thesis, University of Stuttgart.
[38] VOGEL, A. I., 1957, *Practical Organic Chemistry* (Longman Green), p. 745.
[39] MORO, G., and FREED, J. H., 1981, *J. chem. Phys.*, **74**, 3757.
[40] REDFIELD, A. G., 1965, *Adv. magn. Reson.*, **1**, 1.
[41] TORCHIA, D. A., and SZABO, A., 1982, *J. magn. Reson.*, **49**, 107.
[42] LIPARI, G., and SZABO, A., 1982, *J. Am. chem. Soc.*, **104**, 4546.
[43] MANTSCH, H. H., SAITO, H. H., and SMITH, I. C. P., 1977, *Prog. nucl. magn. Reson. Spectrosc.*, **11**, 211.
[44] BOS, P. J., PIRS, J. UKLEIJA, P., DOANE, J. W., and NEUBERT, M. E., 1977, *Molec. Crystals liq. Crystals*, **40**, 59.
[45] DIANOUX, A. J., FERREIRA, J. B., MARTINS, A. F., GIROUD, A. M., and VOLINO, F., 1985, *Molec. Crystals liq. Crystals*, **116**, 319.
[46] SAUPE, A., 1964, *Z. Naturf.* A, **19**, 161.
[47] SHIMIZU, H., 1962, *J. chem. Phys.*, **37**, 765.
[48] BRYAN, R. F., 1967, *J. chem. Soc.* B, p. 1311.
[49] COLAPIETRO, M., and DOMENICANO, A., 1978, *Acta crystallogr.* B, **34**, 3277.
[50] HUMMEL, J. P., and FLORY, P. J., 1980, *Macromolecules*, **13**, 479.
[51] EMSLEY, J. W., HEATON, N. J., KIMMINGS, M. J., and LONGERI, M., 1987, *Molec. Phys.*, **61**, 433.
[52] COUNSELL, C. J. R., EMSLEY, J. W., LUCKHURST, G. R., and SACHDEV, H. S., 1988, *Molec. Phys.*, **63**, 33.
[53] EMSLEY, J. W., LUCKHURST, G. R., and STOCKLEY, C. P., 1982, *Proc. R. Soc. Lond.* A, **381**, 117.
[54] SAMULSKI, E. T., 1983, *Israel J. Chem.*, **23**, 329.
[55] SAMULSKI, E. T. (Private communication).
[56] WASSMER, K.-H., OHMES, E., PORTUGALL, M., RINGSDORF, H., and KOTHE, G., 1985, *J. Am. chem. Soc.*, **107**, 1511.
[57] PSCHORN, U., SPIESS, H. W., HISGEN, B., and RINGSDORF, H., 1986, *Macromol. Chem.*, **187**, 2711.
[58] HSI, S., ZIMMERMANN, H., and LUZ, Z., 1978, *J. chem. Phys.*, **69**, 4126.
[59] GRIFFIN, A. C., and SULLIVAN, S. L., 1988, *Polym. Prepr. Am. chem. Soc.*, **29**, 470.
[60] MÜLLER, K., and KOTHE, G., (to be published).
[61] SCHLEICHER, A., 1985, Diploma Thesis, University of Stuttgart.
[62] SAUPE, A., 1960, *Z. Naturf.* A, **15**, 815.
[63] GRULER, H., SCHEFFER, T. J., and MEIER, G., 1972, *Z. Naturf.* A, **27**, 966.
[64] CASAGRANDE, C., FABRE, P., VEYSSIE, M., WEILL, C., and FINKELMANN, H., 1984, *Molec. Crystals liq. Crystals*, **113**, 193.
[65] DOBB, M. G., and MCINTYRE, J. E., 1984, *Adv. Polym. Sci.*, **60/61**, 61.
[66] CHUNG, T.-S., 1986, *Polym. Engng Sci.*, **26**, 901.
[67] FERRARINI, A., MORO, G., and NORDIO, P. L., 1988, *Molec. Phys.*, **63**, 225.
[68] MEIROVITCH, E., and FREED, J. H., 1980, *J. phys. Chem.*, **84**, 2459.
[69] LUYTEN, P. R., VOLD, R. R., and VOLD, R. L., 1985, *J. phys. Chem.*, **89**, 545.
[70] BECKMANN, P. A., EMSLEY, J. W., LUCKHURST, G. R., and TURNER, D. L., 1986, *Molec. Phys.*, **59**, 97.
[71] NOACK, F., 1986, *Prog. nucl. magn. Reson. Spectrosc.*, **18**, 171.
[72] DONG, R. Y., and RICHARDS, G. M., 1988, *J. chem. Soc. Faraday Trans 2*, **84**, 1053.
[73] DIPPEL, T., SCHWEIKERT, K. H., MÜLLER, K., KOTHE, G., and NOACK, F. (to be published).